Peak Valley Edge Patterns: A New Descriptor for Biomedical Image Indexing and Retrieval

[1]Subrahmanyam Murala, [2]Q. M. Jonathan Wu
Department of Electrical and Computer Engineering,
University of Windsor, Windsor, ON, Canada
[1]muralasu@uwindsor.ca, [2]jwu@uwindsor.ca

Abstract

A new algorithm meant for biomedical image retrieval application is presented in this paper. The local region of image is represented by peak valley edge patterns (PVEP), which are calculated by the first-order derivatives in 0º, 45º, 90º and 135º directions. The PVEP differs from the existing local binary pattern (LBP) in a manner that it extracts the directional edge information based on first-order derivative in an image. Further, the effectiveness of our algorithm is confirmed by combining it with Gabor transform. The performance of the proposed method is tested on VIA/I–ELCAP database which includes region of interest computer tomography (ROI-CT) images. Performance analysis shows that the proposed method improves retrieval results from 79.21% to 86.13% and 51.91% to 55.06% as compared to LBP in terms of average precision when number of top matches considered is 10 and 100 respectively.

1. Introduction

It is observed that there has been a drastic expansion of biomedical images in hospitals and medical institutions in order to meet ones' medical requirement. This huge data exists in different format such as computer tomography (CT), magnetic resonance images (MRI), ultrasound (US), X-ray etc. Handling of these databases by human annotation is an extremely tedious rather impractical task. Hence, there is a dire need of some search technique viz content based image retrieval (CBIR). When we gives patient report (image) as a query the CBIR system retrieves related patients report which has been stored with description about disease as database. With the help of these retrieved reports, we can identify the exact disease in the present patient report. The comprehensive and extensive literature of CBIR is available in [1–6].

Texture based medical image retrieval is a branch of texture analysis particularly well suited for identification of disease region, and then retrieval of related documents in the database is making it a star of attraction from medical prospective. Yang et al. [7] proposed a boosting framework for visuality-preserving distance metric learning for medical image retrieval application. Quellec et al. [8] proposed the optimized wavelet transform for medical image retrieval by adapting the wavelet basis, within the lifting scheme framework for wavelet decomposition. Felipe et al. [9] used the co-occurrence matrix for retrieval of medical CT and MRI images in different tissues.

A concise review of the related literature available, targeted for development of our algorithms is presented. Local binary pattern (LBP) features have emerged as a silver lining in the field of texture retrieval. Ojala et al. proposed LBP [10] further which are converted to rotational invariant [11, 12] for texture classification. The combination of Gabor filter and LBP for texture segmentation [13] and rotational invariant texture classification using LBP variance with global matching [14] has also been reported. Liao et al. [15] proposed the dominant local binary patterns (DLBP) for texture classification. Guo et al. [16] developed the completed LBP (CLBP) scheme for texture classification. Recently LBP has been used in the field of biomedical image retrieval and classification and proved its great success. Peng et al. [17] proposed the texture feature extraction based on a uniformity estimation method in chest CT images. They used the extended rotational invariant LBP and gradient orientation difference to represent brightness and structure in an image. Unay et al. [18] proposed the local structure-based region-of-interest retrieval in brain MR images. Sørensen et al. [19] have done the quantitative analysis of pulmonary emphysema using LBP. They improved the quantitative measures of emphysema in CT images of the lungs by using joint LBP and intensity histograms.

The authors have bestowed the thrust for carrying out the experiments on the following: The PVEP operator is proposed in contrast to the LBP. The combination of Gabor transforms and PVEP is also presented. Further, the performance of the proposed method is experienced for biomedical image retrieval application on region of interest (ROI) CT lunge image database.

The organization of paper is as follows: section 1 provides a brief review of content based image retrieval and related work. Section 2, presents a concise review of

978-0-7695-4990-3/13 $26.00 © 2013 IEEE
DOI 10.1109/CVPRW.2013.73

local binary patterns and peak valley edge patterns (PVEP). Section 3, fetch information about Gabor transform, proposed system framework and query matching. Experimental results and discussions are successfully mentioned in section 4. Based on above work conclusions are derived in section 5.

2. Local Patterns

2.1. Local Binary Patterns (LBP)

The LBP operator was introduced by Ojala et al. [10] for texture classification. Success in terms of speed (no need to tune any parameters) and performance is reported in many research areas such as texture classification [10–16], face recognition [20] and bio-medical image retrieval [17–19]. Given a center pixel in the 3×3 pattern, LBP value is computed by comparing its gray scale value with its neighborhoods based on Eq. (1) and Eq. (2):

$$LBP_{P,R} = \sum_{i=1}^{P} 2^{(i-1)} \times f_1(I(g_i) - I(g_c)) \tag{1}$$

$$f_1(x) = \begin{cases} 1 & x \geq 0 \\ 0 & else \end{cases} \tag{2}$$

where $I(g_c)$ denotes the gray value of the center pixel, $I(g_i)$ is the gray value of its neighbors, P stands for the number of neighbors and R, the radius of the neighborhood.

After computing the LBP pattern for each pixel (j,k), the whole image is represented by building a histogram as shown in Eq. (3)

$$H_{LBP}(l) = \sum_{j=1}^{N_1} \sum_{k=1}^{N_2} f_2(LBP(j,k), l);\ l \in [0, (2^P - 1)] \tag{3}$$

$$f_2(x, y) = \begin{cases} 1 & x = y \\ 0 & else \end{cases} \tag{4}$$

where the size of input image is $N_1 \times N_2$.

Figure 1 shows an example for obtaining an LBP from a given 3×3 pattern. The histograms of these patterns contain the information on the distribution of edges in an image.

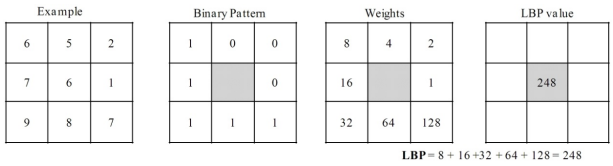

Figure 1: Example of obtaining LBP for the 3×3 pattern

2.2. Peak Valley Edge Patterns (PVEP)

In proposed method (PVEP) for a given image the directional edges in 0º, 45º, 90º and 135º are obtained by local difference between the center pixel and its neighbors as given below:

$$I'(g_i) = I(g_c) - I(g_i);\quad i = 1, 2, ..., 8 \tag{5}$$

The directional edges are obtained by Eq. (6).

$$\hat{I}_\alpha(g_c) = f_3(I'(g_j), I'(g_{j+4})); \quad j = (1 + \alpha/45)\ \forall \alpha = 0^\circ, 45^\circ, 90^\circ \text{ and } 135^\circ \tag{6}$$

$$f_3(I'(g_j), I'(g_{j+4})) = \begin{cases} 1 & I'(g_j)\ \&\ I'(g_{j+4}) \geq 0 \\ 2 & I'(g_j)\ \&\ I'(g_{j+4}) < 0 \\ 0 & else \end{cases} \tag{7}$$

The PVEP is defined (α=0º, 45º, 90º and 135º) as follows:

$$PVEP(I(g_c))\big|_\alpha = \left\{\hat{I}_\alpha(g_c); \hat{I}_\alpha(g_1); \hat{I}_\alpha(g_2); .....\hat{I}_\alpha(g_8)\right\} \tag{8}$$

PVEP is the ternary pattern (0, 1, 2) which is further converted into two binary patterns i.e. peak edge pattern (PEP) and valley edge pattern (VEP). The detailed representation of these two patterns is shown in Figure 2.

Eventually, the given image is converted to PEP and VEP images having values ranging from 0 to 511.

After calculation of PEP and VEP, the whole image is represented by building a histogram supported by Eq. (9).

$$H_{PVEP|_\alpha}(l) = \sum_{j=1}^{N_1} \sum_{k=1}^{N_2} f_2(PVEP(j,k)\big|_\alpha, l);\quad l \in [0, 511] \tag{9}$$

The PVEP computation for a center pixel marked with red color has been illustrated in Figure 2. When the local difference between the center pixel and its eight neighbors are calculated, we obtain directions as shown in Figure 2. Further, these directions are utilized to obtain PVEP ternary patterns in 0º, 45º, 90º and 135º directions. After coding PVEP patterns, we separate them in to two binary patterns as shown in Figure 2. Figure 3 illustrates the possible peak valley patterns in 0º direction. The local pattern is coded to peak pattern when two directions are approaching the center and valley pattern when two directions are leaving from the center as clearly shown in Figure 3.

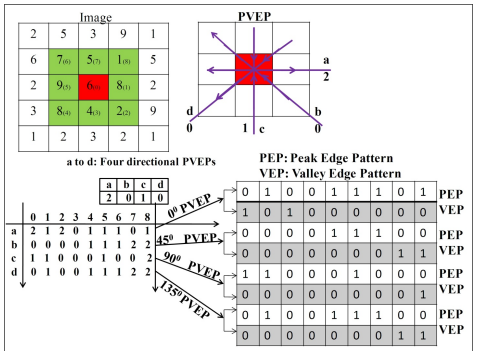

Figure 2: Example of obtaining PEP and VEP for the 3×3 pattern

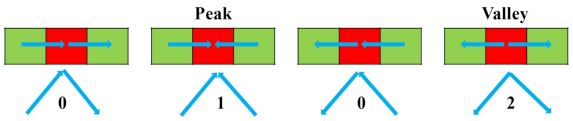

Figure 3: PVEP pattern bits calculation using the directions of pixels

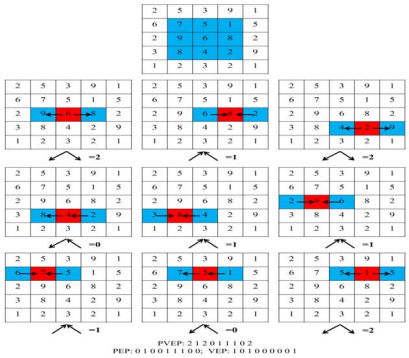
Figure 4: Example to obtain PVEP pattern in 0º direction

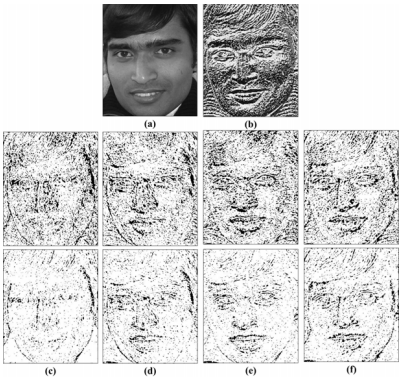
Figure 5: Example of LBP and PVEP feature maps: (a) sample image, (b) LBP feature map, (c) PEP and VEP feature maps in 0º direction, (d) PEP and VEP feature maps in 45º direction, (e) PEP and VEP feature maps in 90º direction (f) PEP and VEP feature maps in 135º direction.

The proposed PVEP is different from the well-known LBP. The PVEP encodes the spatial relation between any pair of neighbors in a local region along a given direction, while LBP [10] extracts relation between the center pixel and its neighbors. Therefore, PVEP captures more edge information as compared to LBP.

An example of the PVEP computation in 0º direction for a center pixel marked with red color has been illustrated in Figure 4. For a center pixel '6' we apply the first order derivative in horizontal direction and then we observe that these two directions are leaving from the center pixel hence this pattern is called valley pattern in 0º direction. Similarly, we computed the remaining bits of PVEP for other 8 neighbors resulting in PVEP ternary pattern that is '2 1 2 0 1 1 1 0 2'. After coding PVEP pattern, we separate them into two binary patterns (PEP and VEP) '0 1 0 0 1 1 1 0 0' and '1 0 1 0 0 0 0 0 1'. Similarly, PVEP patterns for center pixel in the directions 45º, 90º, and 135º are also computed.

Figure 5 illustrates the results obtained by applying LBP and PVEP operators on reference face image. Face image is chosen as it provides the results which are visibly comprehensible to differentiate the effectiveness of these approaches. From Figure 5, it is observed that the PVEP yields more directional edge information as compared to LBP. The experimental results demonstrate that the proposed PVEP shows better performance as compared to LBP, indicating that it can capture more edge information than LBP for texture extraction.

3. Feature Extraction and Similarity Measure

3.1. Gabor Transform

Subrahmanyam et al. [21] has given the spatial implementation of Gabor transform. A 2D Gabor function is a Gaussian modulated by a complex sinusoid. It can be specified by the frequency of the sinusoid ω and the standard deviations σ_x and σ_y of the Gaussian envelope as follows:

$$\psi(x,y)=\frac{1}{2\pi\sigma_x\sigma_y}e^{[-(1/2)(x^2/\sigma_x^2+y^2/\sigma_y^2)+2\pi j\omega x]} \quad (10)$$

The response of Gabor filter is the convolution of Gabor window with image I is given by Eq. (11).

$$G_{mn}(x,y)=\sum_s\sum_t I((\text{x-s, y-t})\psi^*_{\text{mn}}(s,t) \quad (11)$$

3.2. Proposed System Framework

Figure 6 shows the flow chart of the proposed image retrieval system and algorithm for the same is given below:

Algorithm:

Input: Image; Output: Retrieval result

1. Load the gray scale image
2. Calculate the first order-derivatives in 0º, 45º, 90º and 135º directions.
3. Compute the PVEP patterns in 0º, 45º, 90º and 135º directions.
4. Separate PEP and VEP patterns from the PVEP patterns.
5. Construct the histograms for PEP and VEP patterns in 0º, 45º, 90º and 135º directions.
6. Construct the feature vector by concatenating all histograms.
7. Compare the query image with the image in the database using Eq. (12).
8. Retrieve the images based on the best matches.

The above algorithm is applied on the Gabor wavelet (with three scales and four directions) subbands for proposed method with Gabor transform.

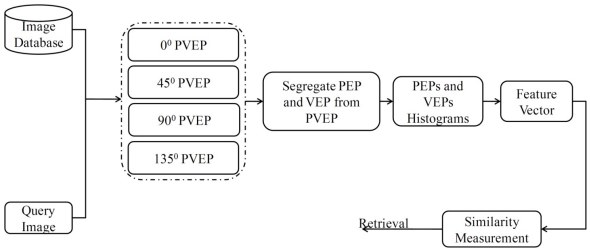

Figure 6: Proposed retrieval system framework

3.3. Query Matching

Feature vector for query image Q is represented as $f_Q = (f_{Q_1}, f_{Q_2}, ...f_{Q_{Lg}})$ obtained after the feature extraction. Similarly, each image in the database is represented with feature vector $f_{DB_i} = (f_{DB_{i1}}, f_{DB_{i2}}, ...f_{DB_{iLg}}); \forall i = 1,2,.....,|DB|$. The goal is to select n best images that resemble the query image. This involves selection of n top matched images by measuring the distance between query image and images in the database $|DB|$. In order to match the images, we used d_1 similarity distance metric computed by Eq. (12).

$$D(Q,DB) = \sum_{i=1}^{Lg} \left| \frac{f_{DB_{ji}} - f_{Q_i}}{1 + f_{DB_{ji}} + f_{Q_i}} \right| \quad (12)$$

where $f_{DB_{ji}}$ is i^{th} feature of j^{th} image in the database $|DB|$.

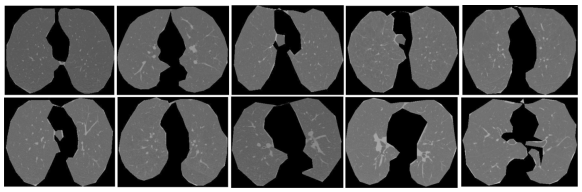

Figure 7: Sample images from VIA/I-ELCAP –CT image database.

4. Experimental Results and Discussions

In order to analyze the performance of proposed method for image retrieval, experimentation is conducted on ROI-CT lunge image database [22] and results obtained are discussed in the following section.

The abbreviations for extracted features are given below:

LBP: *Local Binary Patterns*
PEP: *Peak Edge Patterns*
GLBP: *LBP with Gabor Transform*
VEP: *Valley Edge Patterns*
PVEP: *Peak Valley Edge Patterns*
INTH: *Intensity Histogram* [19]
GLCM1: *Gray Level Co-occurrence Matrix Type 1* (*Autocorrelation*) [19]
GLCM2: *Gray Level Co-occurrence Matrix Type 2* (*Correlation*)[19]
GPVEP: *PVEP with Gabor Transform*
GFB: *First Four Central Moments of Gaussian Filter Bank with Four Scales* [19]

The average retrieval precision (ARP) and average retrieval rate (ARR) judge the performance of the proposed method those are calculated by Eq. (13) − (16).

For the query image I_q, the precision (P) and recall (R) are defined as follows:

$$P(I_q) = \frac{Number\ of\ relevant\ images\ retrieved}{Total\ Number\ of\ images\ retrieved} \quad (13)$$

$$ARP = \frac{1}{|DB|} \sum_{i=1}^{|DB|} P(I_i) \Bigg| \quad (14)$$

$$R(I_q) = \frac{Number\ of\ relevant\ images\ retrieved}{Total\ Number\ of\ relevant\ images\ in\ the\ database} \quad (15)$$

$$ARR = \frac{1}{|DB|} \sum_{i=1}^{|DB|} R(I_i) \Bigg| \quad (16)$$

4.1. VIA/I-ELCAP Dataset

Vision and image analysis (VIA) group and international early lung cancer action program (I-ELCAP) created a computer tomography (CT) dataset [22] for performance evaluation of different computer aided detection systems. These images are in DICOM (digital imaging and communications in medicine) format. The CT scans were obtained in a single breath hold with a 1.25 mm slice thickness. The locations of nodules detected by the radiologist are also provided. The CT scan data acquisition details are given in Table 1. For experiments we have selected 10 scans. Each scan has 100 images with resolution 512×512. Further, ROIs were annotated manually to construct the ROI CT image database. Figure 7 depicts the sample images of VIA/I-ELCAP database (one image from each category).

Table 2 and 3 show the retrieval results of existing methods and proposed method with and without Gabor transform in terms of average precision. The results are considered better, if average value of precision is high.

From Table 2 and 3, the following points are obtained.

1. The ARP (n=10) of proposed method (PVEP) (86.13%) is more as compared to INTH (60.76%), GLCM1 (63.37%), GLCM2 (65.04%), GFB (48.9%), LBP (79.21%), GLBP (84.78%) and GPVEP (85.35%).
2. The ARR (n=100) of proposed method (PVEP) (55.06%) is far better compared to INTH (29.4%), GLCM1 (29.63%), GLCM2 (31.38%), GFB (24.18%), LBP (51.91%), GLBP (50.98%) and GPVEP (54.79%).

Figure 8 (a) – (f) depicts the retrieval performance of

PVEP, GPVEP and other existing methods as function of number of top matches. From Table 2 and 3, Figure 8 and above observations, it is evident that the proposed methods (PVEP and GPVEP) outperform the other existing methods.

5. Conclusions and Feature Scope

A novel method employing PVEP operator in contrast to LBP is proposed in this paper for biomedical image retrieval. The proposed method extracts the edge information from images using direction of edges which are calculated by the first-order derivatives in 0º, 45º, 90º and 135º directions. Further, the combination of Gabor transform and PVEP operators known as GPVEP is proposed. The effectiveness of the proposed method is tested by conducting the experimentation on biomedical ROI-CT image database. The results after investigation show that the proposed method (PVEP) outperforms the LBP, INTH, GLCM1, GLCM2, and GFB on the basis of ARR and ARP.

In this paper, we have considered only P=8 and R=1 for four directional (0º, 45º, 90º and 135º) first order-derivatives calculation. Results can be further improved by considering the P=16 and R=2 for eight directional (0º, 22.5º, 45º, 67.5º, 90º, 112.5º, 135º and 157.5º) first order-derivatives. Due to the effectiveness of our method, we feel that it is also suitable for other pattern recognition applications.

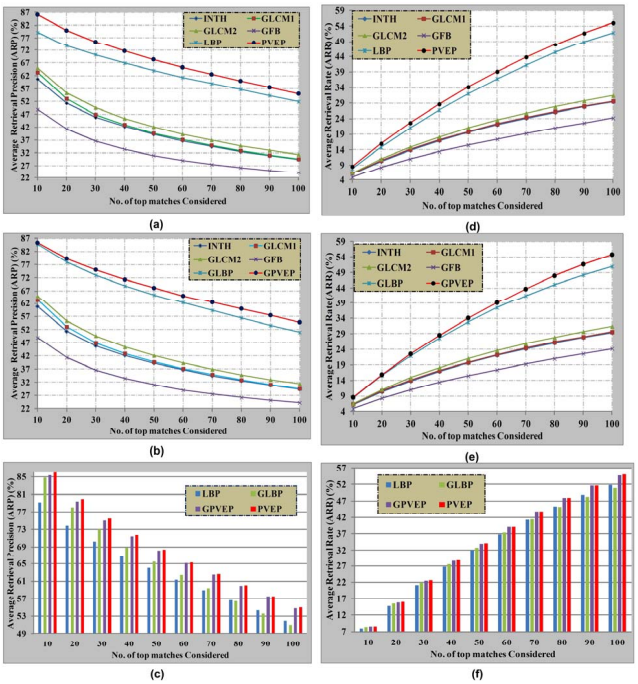

Figure 8: comparison of proposed method with other existing methods in terms of: (a)–(c) average retrieval precision and (d)–(e) average retrieval rate.

Table 1: Data acquisition details of VIA/I-ELCAP –CT lung image database

Data	No. of slices	Resolution	In-plane resolution	Slice thickness (mm)	Tube voltage (kV)
W0001 to W0010	100	512×512	0.76 × 0.76	1.25	120

Table 2: Retrieval results of all techniques in terms of precision (Number of top matches considered n=10)

Group No.	INTH	GLCM1	GLCM2	GFB	LBP	PVEP	GLBP	GPVEP
1	73.1	76.8	49.6	57.9	56.6	68.1	67.8	69.4
2	50.8	55.1	52.6	44	72.7	81.9	84.0	73.7
3	52.4	55.1	58.5	50.3	64.7	80.1	77.8	80.9
4	50.7	54.9	80.8	37.1	89.5	91.2	92.0	91.1
5	46.4	49.9	48.2	37.4	67.8	79.2	79.2	77.9
6	60.5	74.0	77.2	45.4	91.6	97.3	89.3	94.9
7	62.9	68.5	55.0	38.4	80.4	86.0	77.1	91.5
8	94.1	94.7	92.5	90.9	99.7	100	99.1	99.8
9	42.9	32.3	61.5	29.2	78.4	82.7	84.1	78.7
10	73.8	72.4	74.8	58.4	90.7	94.8	97.4	95.6
Total	**60.76**	**63.37**	**65.04**	**48.9**	**79.21**	**86.13**	**84.78**	**85.35**

Table 3: Retrieval results of various techniques in terms of precision/recall (Number of top matches considered n=100)

Group No.	INTH	GLCM1	GLCM2	GFB	LBP	PVEP	GLBP	GPVEP
1	32.2	33.2	23.1	36.4	32.4	35.5	34.5	35.4
2	25.6	28.2	25.8	22.5	40.5	39.7	42.5	39.0
3	17.7	16.5	23.0	18.7	38.6	39.8	41.5	38.8
4	24.4	26.3	52.0	14.7	66.9	64.5	65.9	63.0
5	20.7	19.6	20.5	20.4	36.1	39.6	37.6	38.2
6	29.6	34.1	38.4	23.0	54.2	59.5	51.1	63.0
7	25.3	27.5	22.7	17.7	48.4	54.0	40.2	56.0
8	51.0	52.9	40.9	43.3	81.1	92.2	72.0	87.3
9	19.5	15.4	26.4	13.7	47.8	47.4	47.3	47.0
10	47.5	42.1	40.5	30.9	72.6	77.9	76.7	79.8
Total	**29.4**	**29.6**	**31.3**	**24.1**	**51.9**	**55.0**	**50.9**	**54.8**

References

[1] Deserno T. M., Antani S. and Long R.: Ontology of Gaps in Content-Based Image Retrieval. J. Digital Imaging 22 (2): 202–215 2009.

[2] Smeulders A. W. M., Worring M., Santini S., Gupta A. and Jain R.: Content-Based Image Retrieval at the end of the Early Years. IEEE Trans. Pattern Anal. Mach. Intell., 22 (12): 1349–1380 2000.

[3] Kokare M., Chatterji B. N. and Biswas P. K.: A Survey on Current Content-Based Image Retrieval Methods. IETE J. Res., 48 (3&4): 261–271 2002.

[4] Lew M. S., Sebe N., Djeraba C. and Jain R.: Content-Based Multimedia Information Retrieval: State of the Art and Challenges. ACM Trans. Multimedia Comput., Commun., Appl. 2 (1): 1–19 2006.

[5] Liu Y., Zhang D., Lu G. and Ma W.-Y.: A Survey of Content-Based Image Retrieval with High-Level Semantics. J. Pattern Recognition 40: 262-282 2007.

[6] Muller H., Michoux N., Bandon D. and Geissbuhler A.: A Review of Content-Based Image Retrieval Systems in Medical Applications–Clinical Benefits and Future Directions. J. Med. Inf. 73 (1): 1–23 2004.

[7] Yang L., Jin R., Mummert L., Sukthankar R., Goode A., Zheng B., Hoi S. C.H. and Satyanarayanan M.: A Boosting Framework for Visuality-Preserving Distance Metric Learning and Its Application to Medical Image Retrieval. IEEE Trans. Pattern Anal. Mach. Intell. 32 (1): 33–44 2010.

[8] Quellec G., Lamar M., Cazuguel G., Cochener B. and Roux C.: Wavelet Optimization for Content-Based Image Retrieval in Medical Databases. J. Medical Image Analysis 14: 227–241 2010.

[9] Felipe J. C., Traina A. J. M. and Traina Jr. C.: Retrieval by Content of Medical Images Using Texture for Tissue Identification. 16th IEEE Symp. Comput.-Based Med. Syst., New York, USA 175–180 2003.

[10] Ojala T., Pietikainen M. and Harwood D.: A Comparative Sudy of Texture Measures with Classification Based on Feature Distributions. J. Pattern Recognition 29 (1): 51-59 1996.

[11] Ojala T., Pietikainen M. and Maenpaa T.: Multiresolution Gray-Scale and Rotation Invariant Texture Classification with Local Binary Patterns. IEEE Trans. Pattern Anal. Mach. Intell. 24 (7): 971-987 2002.

[12] Lategahn H., Gross S., Stehle T. and Aach T.: Texture Classification by Modeling Joint Distributions of Local Patterns With Gaussian Mixtures. IEEE Trans. Image Proc. 19(6): 1548–1557 2010.

[13] Li M. and Staunton R. C.: Optimum Gabor Filter Design and Local Binary Patterns for Texture Segmentation. J. Pattern recognition 29: 664-672 2008.

[14] Guo Z., Zhang L. and Zhang D.: Rotation Invariant Texture Classification Using LBP Variance with Global Matching. J. Pattern recognition 43: 706-716 2010.

[15] Liao S., Law M. W. K. and Chung A. C. S.: Dominant Local Binary Patterns for Texture Classification. IEEE Tans. Image Proc. 18 (5): 1107–1118 2009.

[16] Guo Z., Zhang L. and Zhang D.: A Completed Modeling of Local Binary Pattern Operator for Texture Classification. IEEE Tans. Image Proc. 19 (6): 1657–1663 2010.

[17] Peng S.-H., Kim D.-H., Lee S.-L. and Lim M.-K.: Texture Feature Extraction on Uniformity Estimation for Local Brightness and Structure in Chest CT Images. J. Compt. Bilogy amd Medic. 40: 931–942 2010.

[18] Unay D., Ekin A.t and Jasinschi R. S.: Local Structure-Based Region-of-Interest Retrieval in Brain MR Images. IEEE Trans. Infor. Tech. Biomedicine 14 (4): 897–903 2010.

[19] Sørensen L., Shaker S. B. and Bruijne M.: Quantitative Analysis of Pulmonary Emphysema Using Local Binary Patterns. IEEE Trans. Medical Imaging 29 (2): 559–569 2010.

[20] Ahonen T., Hadid A. and Pietikainen M.: Face description with Local Binary Patterns: Applications to Face Recognition. IEEE Trans. Pattern Anal. Mach. Intell. 28 (12): 2037-2041 2006.

[21] Subrahmanyam Murala, Gonde A. B. and Maheshwari R. P.: Color and Texture Features for Image Indexing and Retrieval. IEEE Int. Advance Computing Conf., Patial, India 1411-1416 2009.

[22] VIA/I-ELCAP CT Lung Image Dataset, Available [Online]: http://www.via.cornell.edu/databases/lungdb.html.